Vortical Flows over a LEX-Delta Wing at High Angles of Attack

Young-Ki Lee, Heuy-Dong Kim*
School of Mechanical Engineering, Andong National University, 388 Songcheon-dong, Andong, Kyeongbuk 760-749, Korea

The vortical flows over sharp-edged delta wings with and without a leading edge extension have been investigated using a computational method. Three-dimensional compressible Reynolds-averaged Navier-Stokes equations are solved to provide an understanding of the effects of the angle of attack and the angle of yaw on the development and interaction of vortices and the aerodynamic characteristics of the delta wing at a freestream velocity of 20 m/s. The present computations provide qualitatively reasonable predictions of vortical flow characteristics, compared with past wind tunnel measurements. In the presence of a leading edge extension, a significant change in the suction pressure peak in the chordwise direction is much reduced at a given angle of attack. The leading edge extension can also stabilize the wing vortex on the windward side at angles of yaw, which dominates the vortical flows over yawed delta wings.

Key Words : Angle of Attack, Angle of Yaw, Delta Wing, Leading Edge Extension, Vortical Flow, Vortex Breakdown

Nomenclature

C_p : Specific heat at constant pressure
c : Chord
E : Total energy per unit mass
H : Total enthalpy per unit mass
k : Turbulent kinetic energy
Pr_t : Turbulent Prandtl number
p : Pressure in pascal
s : Local semi-span
T : Temperature in Kelvin
t : Time
u_i : Velocity in the i-th direction
u_i' : Velocity fluctuation in the i-th direction
V : Freestream velocity
x_i : Coordinates in the i-th direction
ε : Turbulent dissipation rate
α : Angle of attack
β : Angle of yaw
μ : Viscosity
μ_t : Turbulent viscosity
ρ : Density
τ_{ij} : Viscous stress tensor

* Corresponding Author,
E-mail : kimhd@andong.ac.kr
TEL : +82-54-820-5622; **FAX** : +82-54-823-5495
School of Mechanical Engineering, Andong National University, 388 Songcheon-dong, Andong, Kyeongbuk 760-749, Korea. (Manuscript **Received** December 26, 2003; **Revised** May 24, 2004)

1. Introduction

Due to the requirement of high maneuverability, modern supersonic combat aircraft have preferably adopted delta wings in order to minimize the influence of a shock wave generated on wing surfaces and thus to maintain the flight stability at supersonic speeds. At low speeds and high angles of attack, however, delta wings can introduce detrimental aerodynamic problems such as a sudden reduction of maneuverability and the generation of induced drag. Moreover, these generally have considerable difficulties in the use of high-lift devices like a flap and special care needs to be taken to avoid stall at take-off or landing with high angles of attack (Erickson et al., 1989 ; Ekaterinaris and Schiff, 1993). As delta wings generally have considerable flight

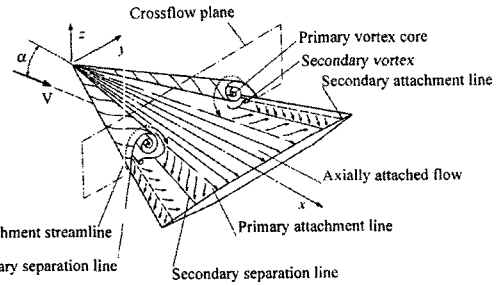

Fig. 1 Schematic diagram of the subsonic flowfield over a delta wing

time at subsonic speeds, the low speed aerodynamics of delta wings is also of great importance in consideration of the high-angle-of-attack controllability and maneuvering effectiveness of aircraft.

Figure 1 shows a typical subsonic flowfield over the upper surface of a delta wing at a freestream velocity V and an angle of attack α. Relatively higher pressure on the bottom plane causes the flow in the vicinity of the leading edge to roll up towards the top plane. Then, the rotating flow separates from the wing due to the effect of the sharp leading edge and produces the primary vortex. As shown in the figure, the vortex reattaches along the primary attachment line and then secondarily separates and reattaches below the primary vortex, forming an oppositely rotating secondary vortex (Hummel, 1978). The leading-edge vortex consequently dominates the overall flowfields on the delta wing. At moderate to high angles of attack, the vortices induce large suction on the wing and thus produce a significant vortex-lift increment. Beyond a critical angle of attack, however, the vortices undergo a sudden expansion, called vortex breakdown (Wentz and Kohlman, 1971), resulting in a significant loss of lift, a sudden change of pitching moment and buffeting.

Since the 1950s, in order to understand the flow physics around various types of delta wings at high angles of attack, considerable effort has been made through experimental and numerical methodologies. Verhaagen et al.(1989) studied the influence of yaw on the flow over a sharp-edged biconvex delta wing at a constant angle of attack of 21.1° through laserlight sheet and oil-flow visualization techniques, and pressure and force balance measurements. Grismer at al. (1995) experimentally investigated the aerodynamic characteristics of a yawed delta wing with the strake at both static and sinusoidally varying angles of attack. Lowson et al.(1995) examined the effects of delta wing configurations, especially apex geometries, on the position of vortex breakdown. Lee and Sohn (2003) investigated vortical flows over a delta wing with a leading edge extension through wing-surface pressure measurements, off-surface flow visualizations and 5-hole probe measurements of a wing wake section. Recently, several Navier-Stokes computations (Fujii and Schiff, 1989; Ekaterinaris and Schiff, 1990; Ken, 1993; Robinson et al., 1994; Gortz et al., 1999) have been conducted to predict separation and vortex breakdown and to find practical control techniques of these phenomena. These studies gave a good understanding of the flow features existing around yawed delta wings or double-delta wings. The experimental studies, however, could not provide comprehensive data to examine the detailed physics of vortical flow due to the difficulty in visualizing the flow structure. Furthermore, there have been rather limited numerical studies which can give quantitative information regarding the vortical flow and its relation to the aerodynamic load characteristics of the yawed delta wings at high angles of attack.

In the present study, three-dimensional compressible Navier-Stokes simulations were carried out to give a detailed understanding of the vortex flow characteristics of simple sharp-edged delta wings with and without LEX (leading edge extension). The results obtained from the present computations were compared with the experimental data (Sohn and Lee, 2002; Kim et al., 2003) and gave the visualization of path lines, density and total pressure contours, vorticity, particle trajectory, etc. which can be hardly disclosed by experimental work.

2. Model Configuration

Figure 2 shows the schematic diagrams of delta

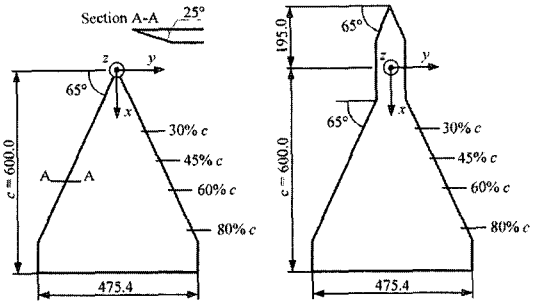

(a) Without LEX (b) With LEX)

Fig. 2 Schematic diagram of delta wing models (units : mm)

wing models (Sohn and Lee, 2002 ; Kim et al., 2003) with and without LEX tested in the present CFD analysis. The present wing models are, basically, a flat type wing with a chord of 600 mm, a span of 475.4 mm at the trailing edge, a sweepback angle of 65° and a thickness of 15 mm. The leading edge of the wing has a bevel angle of 25°. In the Cartesian coordinate system, x is the chordwise distance along the wing centerline measured from the wing apex, y is the spanwise distance measured from the wing centerline and z is the normal distance from the wing upper surface to the freestream. The origin of the coordinate system is the apex of the delta wing and several chordwise locations, 30%, 45%, 60% and 80% of c (c : chord length), were predefined to observe the development of vortices. For the LEX-delta wing, the root chord is 600 mm and the length between the leading edge and the origin is 195 mm.

3. Numerical Simulations

3.1 Governing equations

Three-dimensional Reynolds-averaged Navier-Stokes and energy equations governing the flowfield around delta wings are given in differential form as follows.

$$\frac{\partial \rho}{\partial t}+\frac{\partial}{\partial x_i}(\rho u_i)=0 \tag{1}$$

$$\frac{\partial}{\partial t}(\rho u_i)+\frac{\partial}{\partial x_j}(\rho u_i u_j) =\frac{\partial}{\partial x_j}\mu\left(\frac{\partial u_i}{\partial x_j}+\frac{\partial u_j}{\partial x_i}\right)-\frac{\partial}{\partial x_i}\left(\frac{2}{3}\mu\frac{\partial u_l}{\partial x_l}\right)-\frac{\partial p}{\partial x_i}+\frac{\partial}{\partial x_j}(-\rho\overline{u_i' u_j'}) \tag{2}$$

$$\frac{\partial}{\partial t}(\rho E)+\frac{\partial}{\partial x_i}(\rho u_i H) =\frac{\partial}{\partial x_i}\left[\left(\kappa+\frac{\mu_t}{\mathrm{Pr}_t}\right)\frac{\partial T}{\partial x_i}+u_j(\tau_{ij})_{eff}\right] \tag{3}$$

In Eq. (3), the total enthalpy per unit mass H is related to the total energy per unit mass E by $H=E+p/\rho$, where E includes both internal and kinetic energy. In the term representing the viscous heating, $(\tau_{ij})_{eff}$ is given as

$$(\tau_{ij})_{eff}=\mu_{eff}\left(\frac{\partial u_j}{\partial x_i}+\frac{\partial u_i}{\partial x_j}\right)-\frac{2}{3}\mu_{eff}\frac{\partial u_i}{\partial x_i}\delta_{ij} \tag{4}$$

where μ_{eff} is the effective viscosity ($=\mu+\mu_t$) and δ_{ij} is the Kronecker delta.

The governing equations are discretized spatially using a fully implicit finite volume scheme, in which the physical domain is subdivided into numerical cells and the integral equations are applied to each cell. The flowfield is represented by associating a distinct value of the discretized solution vector with each control volume, which is then used to evaluate the fluxes at cell faces. The solution vector is computed using a multidimensional linear reconstruction approach (Barth and Jespersen, 1989), which enables higher-order accuracy to be achieved at the cell faces through a Taylor series expansion of the cell-averaged solution vector. In the present computations, second order accuracy was applied to solutions in consideration of computational time. With respect to temporal discretization, a 4-stage Runge-Kutta scheme (Jameson et al., 1981) is used to discretize the time derivatives in the governing equations. Then it is assumed that time marching proceeds until a steady state solution is reached.

The standard k-ε turbulence model (Launder and Spalding, 1972), modified to take account of the compressibility effect, was employed to close Eq. (2). The compressibility effect is included in the dilatation term of the turbulence model by the introduction of the turbulent Mach number $M_t=(k/a^2)^{0.5}$ (Sarkar and Balakrishnan, 1990). The model for the turbulent viscosity μ_t is written as $\mu_t=\rho C_\mu(k^2/\varepsilon)$, where the turbulent kinetic energy k and dissipation rate ε are solved from the turbulent transport theory.

The following model constants are used: C_μ= 0.09, $C_{1\varepsilon}$=1.44, $C_{2\varepsilon}$=1.92, σ_k=1.0 and σ_ε=1.3.

3.2 Computational domain and grids

Figure 3 shows the layout of the near-field grids around the delta wing model with LEX and the entire computational domain used in the present study. The three-dimensional structured grid system was used to simulate the vortical flow over delta wings and node points are about 800,000. The grid size was chosen through preliminary grid refinement tests to obtain reliable solutions. Grids were clustered in the regions near the wing surfaces and the sharp leading edge where flow separation can occur, in order to provide accurate predictions of vortex structures. For the standard k-ε model with the standard wall function, y+ numbers used in the present computations are in the range of 50 to 200. To obtain domain-independent solutions, external boundaries were extended by the distance of $6c$ upstream of the apex, $15c$ downstream of the trailing edge and $8c$ spanwise from both sides of the model. For the cases without yaw, especially, computations were conducted only for the right side of the model axis in consideration of symmetry.

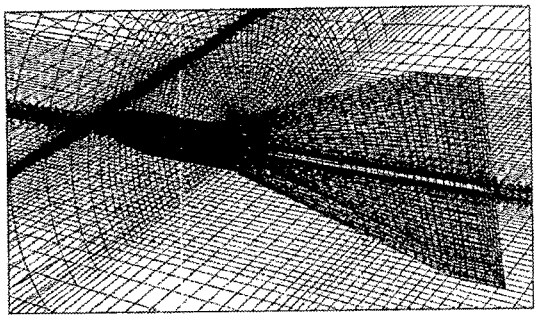

(a) Layout of near-field grids around a LEX-delta wing

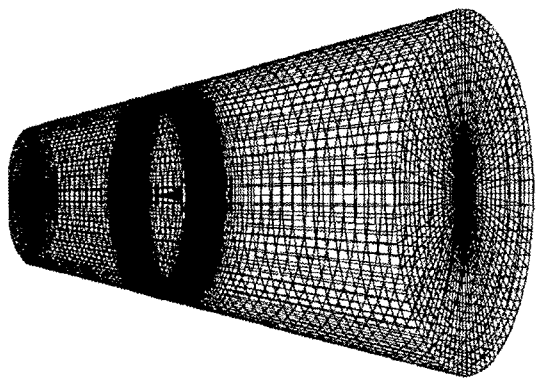

(b) Layout of the entire computational domain

Fig. 3 Computational grid system

3.3 Boundary conditions and analysis

The velocity inlet, pressure outlet and far-field boundary conditions were applied to the upstream boundary, downstream boundary and circumferential boundary respectively, comprising external boundaries of the computational domain. For the velocity inlet boundary condition, a velocity and static temperature were used, and the direction of the velocity was changed according to the angles of attack and angles of yaw under consideration. A uniform static pressure was specified at the pressure outlet boundary, which was set up at a downstream location far from the model to ensure the uniformity. Regarding the far-field boundaries, to describe freestream conditions, the freestream Mach number and static properties were specified. For wing surfaces, no-slip and adiabatic wall conditions were used.

For the testing conditions in the present CFD study, the angle of attack α and the angle of yaw β were changed in the range of $10°\sim30°$ and $0°\sim20°$ respectively at a fixed freestream velocity of 20 m/s. The corresponding Reynolds number based on the freestream velocity and the wing chord length was about 8.2×10^5. A convergence criterion of solutions was established when each residual of conservation equations dropped to 1.0×10^{-4}. When the criterion was satisfied and a change in the force coefficient of the delta wing was less than 0.3%, solutions were considered converged.

4. Results

4.1 Effect of LEX on the development of vortices

At α=24°, β=0° and V=20 m/s, Fig. 4 visualizes typical vortex flows over the upper surfaces of delta wing models with and without

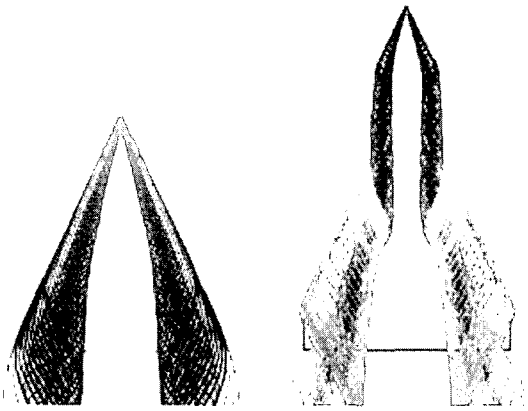

(a) Without LEX (b) With LEX

Fig. 4 Path lines for vortical flows over delta wings

LEX, using the path lines for the particles traced from the sharp leading edge. Without LEX, the fundamental structure of the vortex system is built up in a typical subsonic vortical flowfield. A strong vortex pair develops from the leading edge of the wing due to a large pressure difference between lower and upper surfaces. Then the vortical flow spreads out gradually towards the trailing edge with increased dimensions and consequently breaks down out of the wing surface. In the presence of LEX, another vortex pair, called LEX vortices, is generated in the wake region over the upper wing surface. The vortices developing in the LEX region are just slightly diffused and thus the structure of the vortical flow is maintained up to the trailing edge of the wing.

For the same flight condition, Fig. 5 shows spanwise static pressure distributions on the upper surfaces of the delta wing models. In order to understand the development of vortical flow, the distributions were obtained at the chordwise locations of $x/c=0.3$, 0.6 and 0.8. The computed results are given with measured pressure distributions, taken from the past wind tunnel experiments (Sohn and Lee, 2002; Kim et al., 2003) performed by KAFA (Korean Air Force Academy). In the figure, C_p is static pressure coefficient defined by $C_p \equiv (p-p_\infty)/(\rho_\infty V^2/2)$, where p_∞ is the freestream pressure, and the spanwise distance y is normalized by the local semi-span s of delta wing models. Without LEX, there is

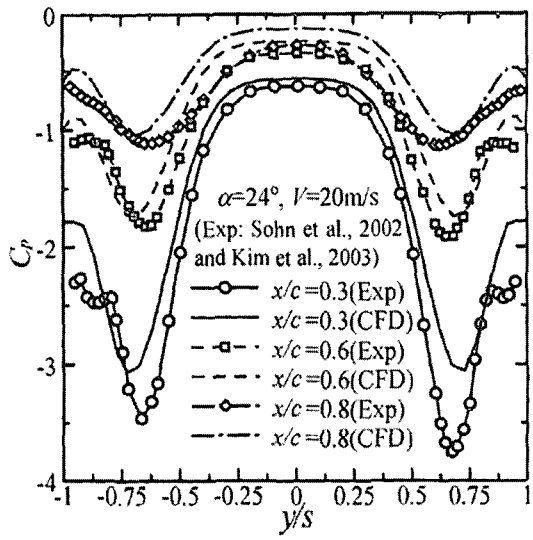

(a) Without LEX

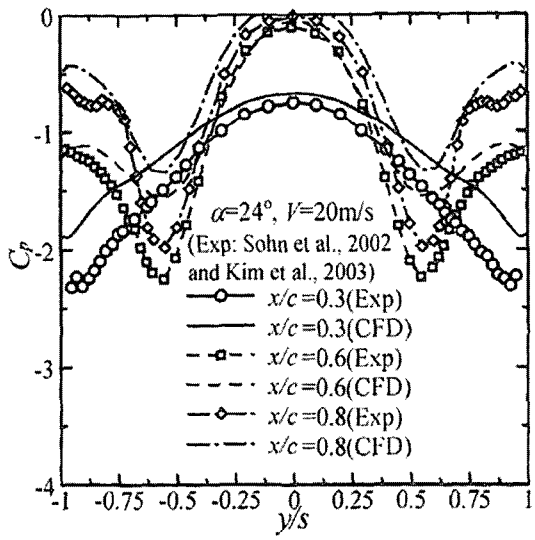

(b) With LEX

Fig. 5 Wing surface pressure distributions at several chordwise locations (α=24° and V=20 m/s)

an absolute peak value of the pressure coefficient, called the suction pressure peak, observed at all chordwise locations and the largest suction pressure peak of computed distributions ($C_p=-3.1$ at $y/s=\pm 0.7$) occurs at an upstream location of $x/c=0.3$. As x/c increases, the suction pressure peak becomes weaker with a reduced gradient due to the diffusion of leading edge vortices along the chordwise direction. With LEX,

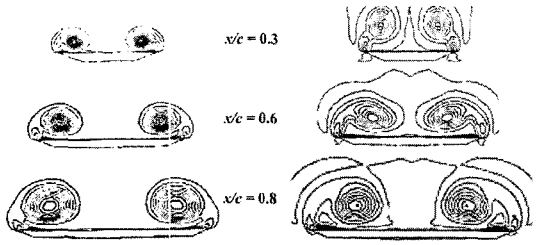

(a) Without LEX (b) With LEX

Fig. 6 Total pressure coefficient contours at several chordwise locations (α=24° and V=20 m/s)

the change in the suction pressure peak is relatively insignificant. It is interesting to note that the pressure distribution at x/c=0.3 has a significantly different gradient from those at downstream locations (x/c=0.6 and 0.8) and the suction pressure peak occurs at an outboard location of the wing (C_p=−1.8 at y/s=±0.95). In this situation, the highest suction pressure peak is observed at x/c=0.6 due to the interaction between LEX vortices and wing vortices. The present computations somewhat underpredict pressure values when compared with the wind tunnel test results but the location of the suction pressure peak and the effect of LEX on the aerodynamic characteristics of the delta wing can be reasonably predicted.

Figure 6 shows total pressure coefficient contours obtained at x/c=0.3, 0.6 and 0.8. The total pressure coefficient C_{pt}, defined by $C_{pt} \equiv (p_t - p_\infty)/(\rho_\infty V^2/2)$, is the most useful non-dimensional property to understand the characteristics of vortex structures and to evaluate a total pressure loss of wake flow. Referring to Crocco's theorem (Liepmann and Roshko, 1957), total pressure gradients are related to vorticity and thus iso-total pressure lines can be used to represent vortices. At a chordwise location close to the trailing edge of the wing without LEX, the C_{pt} gradient near the vortex core is relatively weaker and the wing vortex becomes more widely spread. For the LEX delta wing model, at the 30% chord location, two vortex cores are clearly observed. The upper and lower cores represent the LEX vortices and wing vortices, respectively. At the 60% chord location, LEX vortices move

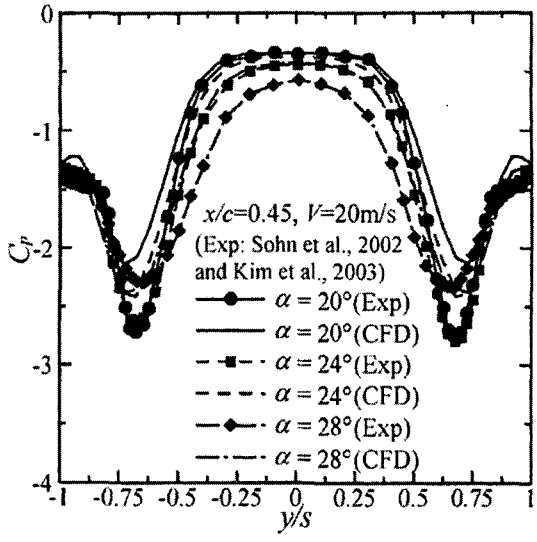

(a) Without LEX

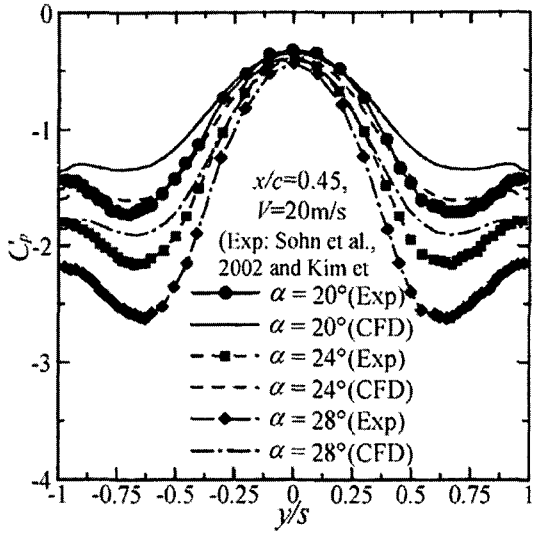

(b) With LEX

Fig. 7 Effects of the angle of attack on surface pressure distributions (x/c=0.45 and V=20 m/s)

inboard and downward, and the interactions between LEX vortices and wing vortices lead to the inboard movement of wing vortices. Near the trailing edge of the wing (x/c=0.8), these vortices completely coalesce into single vortices, resulting in an increase in the suction pressure peak when compared with the LEX-off model (see Fig. 5).

The spanwise pressure distributions obtained

at $x/c=0.45$ and $V=20$ m/s in Fig. 7 show the effect of the angle of attack on the aerodynamic characteristics of the wing models with and without LEX. For the experimental results of the LEX-off model, as α changes from 20° to 24°, the suction pressure peak at a vortex core changes insignificantly but a further increase in α results in a reduced peak value and relatively weaker spanwise pressure gradient. It implies that the vortex-spread rate in the chordwise direction may become suddenly high from a certain angle of attack when it is increasing. However, the present computations do not appropriately predict this behavior due to the weakness of the present turbulence model to predict the sharp pressure changes. It is considered that the Boussinesq approximation (Hinze, 1975) involved in the standard k-ε turbulence model yields a too strong turbulent viscosity in the core of vortices. For the LEX-on model, computed pressure distributions overpredict suction pressure peaks but give qualitatively proper predictions of the aerodynamic characteristics. With LEX, there is no sudden change in vortical flow characteristic as α increases, which was shown for the LEX-off model. It implies that LEX can help stabilize wing vortices developing over delta wings at high angles of attack.

4.2 Vortical flow over a yawed LEX-delta wing

The aerodynamic load of delta wings at high angles of attack is dominated by the suction pressure acting on the upper wing surface and this pressure is mainly attributed to the strong leading edge vortex developing on the wing models (Lee and Kim, 2004). Through the results at zero angle of yaw, it has been found that intense and concentrated leading edge vortices led to pressure distributions with a high suction pressure peak and a large spanwise gradient. In the presence of LEX, wing vortices could be stabilized at high angles of attack. The following figures can explain the effect of yaw on the aerodynamic load characteristics of the LEX-delta wing model.

At $\alpha=20°$, $\beta=10°$ and $V=20$ m/s, Fig. 8 shows

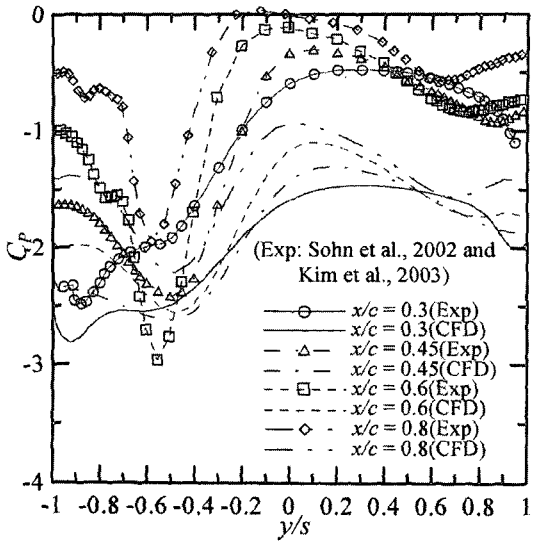

Fig. 8 Wing surface pressure distributions at several chordwise locations ($\alpha=20°$, $\beta=10°$ and $V=20$ m/s)

spanwise pressure distributions at the chordwise locations of $x/c=0.3$, 0.45, 0.6 and 0.8 on the upper surface of the LEX-on model. When compared with the no-yawed case in Fig. 5(b), a yaw angle of 10° completely destroys the symmetry of the vortex pair. In this situation, the suction pressure peak and large pressure gradients are observed on the windward side. At $x/c=0.3$, the suction pressure peak of the experimental result occurs at $y/s=-0.9$. Between $x/c=0.3$ and 0.45, the location of the peak abruptly moves inboard ($\Delta y/s=0.4$) and then it changes insignificantly at further downstream chordwise locations. The largest suction pressure peak occurs at $x/c=0.6$, where considerable interactions between LEX vortices and wing vortices exist. On the leeward side, along the chordwise direction, the suction pressure peak becomes weaker and the location moves inboard monotonically. From this result, it is considered that the present CFD code well predicted the overall aerodynamic load characteristics except the sharp suction pressure peaks at $x/c=0.6$ and 0.8.

For the same angle of attack and freestream velocity, the spanwise pressure distributions obtained at $x/c=0.45$ in Fig. 9 show the effect of

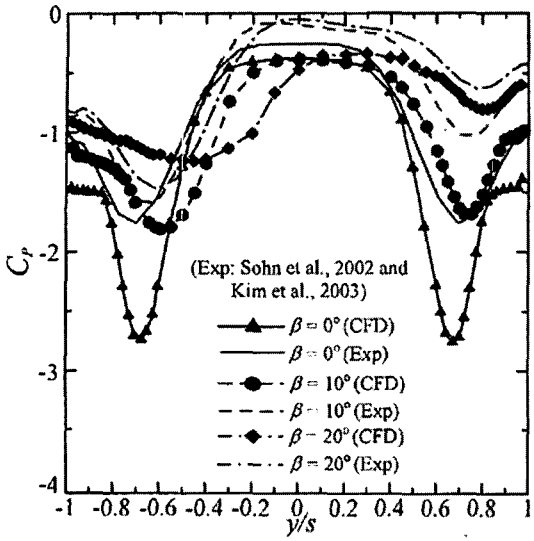

(a) Without LEX

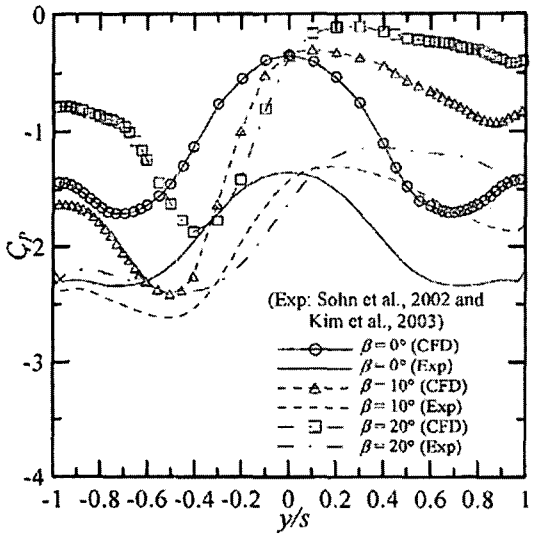

(b) With LEX

Fig. 9 Wing surface pressure distributions with angles of yaw (α=20°, x/c=0.45 and V=20 m/s)

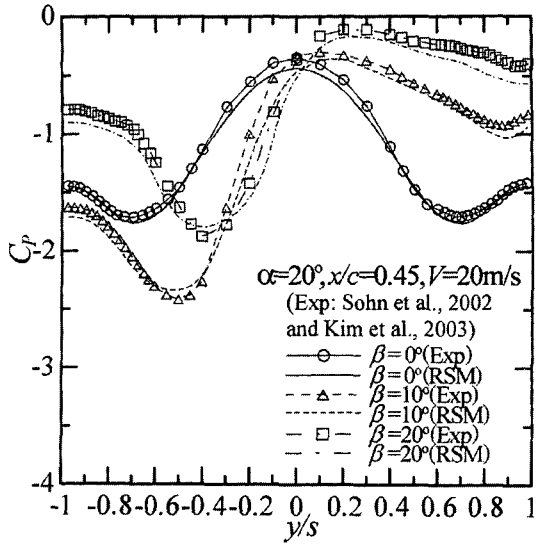

Fig. 10 Spanwise pressure distributions of LEX-on cases with angles of yaw, predicted by RSM (α=20°, x/c=0.45 and V=20 m/s)

the angle of yaw on the aerodynamic load characteristics of delta wing models. For both models, as β increases, the symmetry of a vortex pair at β=0° is broken and asymmetry becomes severe. When the LEX-off model is yawed, there is a considerable reduction in the suction pressure peak observed on the windward side and the vortices on the leeward side are also strongly developed. On the other hand, in the presence of LEX, the change in the suction pressure peak with β on the windward side is relatively insignificant and the vorticies on the leeward side are restrained from developing strongly. It implies that the use of LEX can alleviate vortex break down on the windward side for the angles of yaw tested.

From the present numerical results, it has been considered that the severe deviations from experimental results shown in all pressure distributions could mainly be attributed to the lack of the ability of the k-ε turbulence model to correctly predict strong vortices. In order to prove this fact, the results given in Fig. 9(b) have been validated using a five-equation turbulence model, the Raynolds Stress Model (RSM ; Launder et al., 1975), which is not based on the Boussinesq approximation. For the given testing conditions, in Fig. 10, RSM provides considerably improved predictions of the surface pressure distributions quantitatively as well as qualitatively, compared with those of the standard k-ε turbulence model. Therefore, it is concluded that the use of a proper closure model is essential to provide an insight into the physics of vortical flows over a delta wing.

At α=20° and V=20 m/s, Figs. 11 and 12

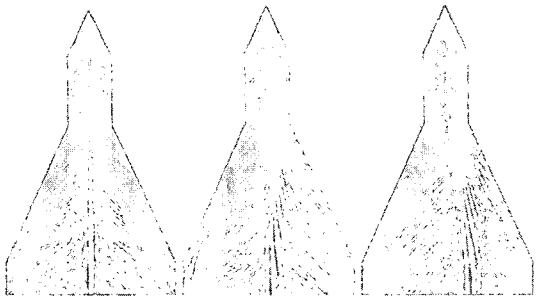

(a) $\beta=0°$ (b) $\beta=10°$ (c) $\beta=20°$

Fig. 11 Computed oilflow patterns at angles of yaw ($\alpha=20°$ and $V=20$ m/s)

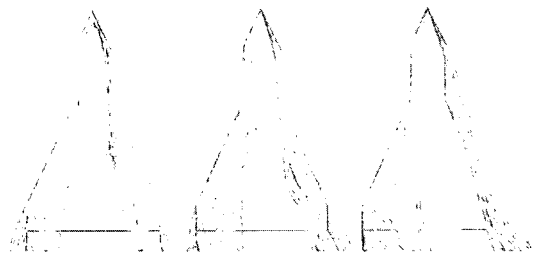

(a) $\beta=0°$ (b) $\beta=10°$ (c) $\beta=20°$

Fig. 12 Path lines at angles of yaw ($\alpha=20°$ and $V=20$ m/s)

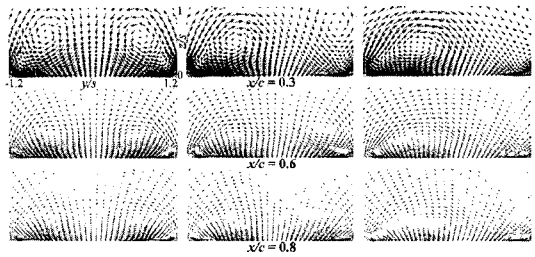

(a) $\beta=0°$ (b) $\beta=10°$ (c) $\beta=20°$

Fig. 13 Velocity vectors at several chordwise cross sections ($\alpha=20°$ and $V=20$ m/s)

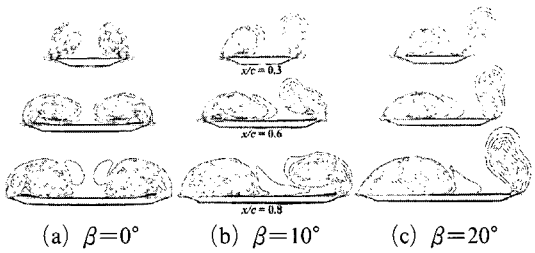

(a) $\beta=0°$ (b) $\beta=10°$ (c) $\beta=20°$

Fig. 14 Total pressure contours at several chordwise locations ($\alpha=20°$ and $V=20$ m/s)

present the computed oilflow visualization and path lines of vortical flows over the upper surface of the LEX-on model with and without yaw. The present computational method predicts well the typical subsonic delta wing flow, such as the separation and reattachment of vortex sheets, as schematically shown in Fig. 1. The dark color in the oilflows represents low-pressure regions. As the angle of yaw increases, LEX vortices and wing vortices move inboard on the windward side and outboard on the leeward side. It can be observed that the LEX vortex interacts strongly with the wing vortex on the windward and the vortex structure is maintained up to the trailing edge. On the leeward side, however, wing vortices quickly spread out at angles of yaw due to the much weaker vortex interaction compared with the case at zero angle of yaw. At a high angle of yaw, $\beta=20°$, the reattachment region of the primary vortex on the windward side is much larger. It implies that the vortical flow on the windward side, which is stabilized by LEX, may govern the aerodynamic characteristics of a yawed LEX-delta wing.

The velocity vectors and total pressure contours for the same flight condition, given in Figs. 13 and 14 respectively, can give an detailed understanding of the vortex development along the chordwise direction on both sides of the LEX-on model with and without yaw. The results are presented at the cross sections of the chordwise locations of $x/c=0.3$, 0.6 and 0.8. Velocity vectors are given in a cross section normalized by the local semi-span s. In both figures, the vortex core is shown as the center of rotating flow vectors and total pressure contours, and the vortex diffusion towards the trailing edge can be clearly observed. The inboard and downward movement of the LEX vortex leads to the coiling of the wing vortex inwards and both vortices coalesce completely at $x/c=0.8$ on the windward side for all yaw angles. On the leeward side, the location of the LEX vortex at angles of yaw are much detached from the wing surface and consequently it does not clearly merge with the wing vortex even near the trailing edge at $\beta=20°$. The strong

vortices on the windward side last up to the trailing edge and these are dominant at angles of yaw. In general, larger lift can be obtained as the vortex strength increases and the vortex core is closer to the suction suface. Therefore, it is considered that these stabilized vortices with LEX can enhance the flight performance of delta wings at angles of yaw.

5. Conclusions

The physics of vortex development and aerodynamic load characteristics of delta wings with and without a leading edge extension have been studied using a computational method. Three-dimensional compressible Navier-Stokes equations with the standard k-ε turbulence model were solved to simulate complex vortical flows using an implicit finite volume scheme and a 4-stage Runge-Kutta scheme. The basic configuration of wing models is a flat type with a chord of 600 mm and a sweepback angle of 65°, which is employed to validate the results obtained through the present CFD analysis with past wind tunnel tests. Various vortical flow features were investigated particularly at high angles of attack with and without yaw.

The spanwise distributions obtained from the present computations gave qualitatively reasonable predictions of the effect of LEX on the aerodynamic load characteristics of delta wings. Several numerical visualization methods provided a good understanding of the fundamental structure of the vortex system developing in the chordwise direction. With LEX, a change in the suction pressure peak in the chordwise direction was relatively insignificant at an angle of attack when compared with the result for the LEX-off model. At angles of yaw, the strong vortices on the windward side were maintained up to the trailing edge and dominated the vortical flows over the upper surface of the LEX-on model. Therefore, a leading edge extension could stabilize the vortices developing over a delta wing at angles of attack and angles of yaw, consequently enhancing the flight performance.

References

Barth, T. J. and Jespersen, D., 1989, "The Design and Application of Upwind Schemes on Unstructured Meshes," *AIAA Paper* 89-0366.

Ekaterinaris, J. A. and Schiff, L. B., 1990, "Numerical Simulation of the Effects of Variation of Angle of Attack and Sweep Angle on Vortex Breakdown over Delta Wings," *AIAA Paper* 90-3000.

Ekaterinaris, J. A. and Schiff, L. B., 1993, "Numerical Predictions of Vortical Flows over Slender Delta Wings," *J. Aircraft*, Vol. 30, pp. 935~942.

Erickson, G. E., Schreiner, J. A. and Roges, L. W., 1989, "On the Structure, Interaction, and Breakdown Characteristics of Slender Wing Vortices at Subsonic, Transonic, and Supersonic Speeds," *AIAA Paper* 89-3345.

Fujii, K. and Schiff, L. B., 1989, "Numerical Simulation of Vortical Flows over Strake-Delta Wing," *AIAA J.*, Vol. 27, pp. 1153~1162.

Gortz, S., Rizzi, A. and Munukka, K., 1999, "Computational Study of Vortex Breakdown over Swept Delta Wings," *AIAA Paper* 99-3118.

Grismer, D. S., 1995, "Double-Delta-Wing Aerodynamics for Pitching Motions with and without Sideslip," *J. Aircraft*, Vol. 32, pp. 1303~1311.

Hinze, J. O., 1975, *Turbulence*, McGraw-Hill Publishing Co., New York, p. 23.

Hummel, D., 1978, "On the Vortex Formation Over a Slender Wing at Large Angles of Incidence," *AGARD-CPP*-247.

Jameson, A., Schmidt, W. and Turkel, E., 1981, "Numerical Solution of the Euler Equations by Finite Volume Methods Using Runge-Kutta Time-Stepping Schemes," *AIAA Paper* 81-1259.

Ken, C., 1993, "Numerical Study of Blowing on Delta Wings at High Alpha," *J. Aircraft*, Vol. 30, pp. 833~839.

Kim, T. H., Kweon, Y. H., Kim, H. D. and Sohn, M. H., 2003, "A Study of the Vortical Flow over a Delta Wing with a Leading Edge Extension," *6th Int. Symposium on Experimental and Computational Aerothermodynamics of In-*

ternal Flows, Shanghai, China, pp. 408~413.

Launder, B. E., Reece, G. J. and Rodi, W., 1975, "Progress in the Development of a Reynolds-Stress Turbulence Closure," *J. Fluid Mech.*, Vol. 68, pp. 537~566.

Launder, B. E. and Spalding, D. B., 1972, *Lectures in Mathematical Models of Turbulence*, Academic Press, London, England.

Lee, K. Y. and Sohn, M. H., 2003, "The Vortical Flow Field of Delta Wing with Leading Edge Extension," *KSME Intl. J.*, Vol. 17, pp. 914~924.

Lee, Y. K. and Kim, H. D., 2004, "Vortical Flows over a Delta Wing at High Angles of Attack," *KSME Intl. J.*, Vol. 18, pp. 1060~1068.

Liepmann, H. W., Roshko, A., 1957, *Elements of Gasdynamics*, John Wiley and Sons, International Edition, pp. 191-193.

Lowson, M. V. and Riley, A. J., 1995, "Vortex Breakdown Control by Delta Wing Geometry," *J. Aircraft*, Vol. 32, pp. 832~838.

Robinson, B. A., Barnett, R. M. and Agrawal, S., 1994, "Simple Numerical Criterion for Vortex Breakdown," *AIAA J.*, Vol. 32, pp. 116~122.

Sarkar, S. and Balakrishnan, L., 1990, "Application of a Reynolds-Stress Turbulence Model to the Compressible Shear Layer," *ICASE Report* 90-18, NASA CR-182002.

Sohn, M. H. and Lee, K. Y., 2002, "Experimental Investigation of Vortex Flow of a Yawed Delta Wing Having Leading Edge Extension," *AIAA paper* 2002-3267.

Verhaagen, N. G. and Naarding, S. H. J., 1989, "Experimental and Numerical Investigation of the Vortex Flow over a Sidesliping Delta Wing," *J. Aircraft*, Vol. 26, pp. 971~978.

Wentz, W. H. Jr. and Kohlman, D. L., 1971, "Vortex Breakdown on Slender Sharp Edged Wings," *J. Aircraft*, Vol. 8, pp. 156~161.